

MELEP: A Novel Predictive Measure of Transferability in Multi-Label ECG Analysis

Cuong V. Nguyen¹, Hieu Minh Duong¹, Cuong D. Do^{1,2}

¹ College of Engineering and Computer Science, VinUniversity, Hanoi, Vietnam

² VinUni-Illinois Smart Health Center, VinUniversity, Hanoi, Vietnam
{cuong.nv, hieu.dm, cuong.dd}@vinuni.edu.vn

ABSTRACT

We introduce MELEP, which stands for *Multi-label Expected Log of Empirical Predictions*, a novel measure to estimate how effective it is to transfer knowledge from a pre-trained model to a downstream task in a multi-label settings. The measure is generic to work with new target data having a different label set from source data. It is also computationally efficient, only requires forward passing the downstream dataset through the pre-trained model once. To the best of our knowledge, we are the first to develop such a transferability metric for multi-label ECG classification problems. Our experiments show that MELEP can predict the performance of pre-trained convolutional and recurrent deep neural networks, on small and imbalanced ECG data. Specifically, strong correlation coefficients, with absolute values exceeding 0.6 in most cases, were observed between MELEP and the actual average F1 scores of the fine-tuned models.

Index Terms— Transfer learning, electrocardiography, multi-label data, pre-transfer evaluation, decision support systems.

1. INTRODUCTION

Automatic ECG interpretation has gained significant popularity and witnessed remarkable progress in recent years. This advancement can be attributed to the wide-scale digitization of ECG data and the evolution of deep learning techniques. Notably, deep neural networks (DNN) have achieved classification performance on par with cardiologists, as demonstrated by Hannun et al. [1], and Ribeiro et al. [2]. These outstanding achievements have partly been due to the availability of extensive human-labeled datasets, consisting of 91,232 and 2,322,513 ECG recordings, respectively. However, ECG datasets used in practice are often much smaller, due to the expensive and time-consuming data collection and annotation process. Consequently, it becomes

challenging to achieve desirable results when training DNNs from scratch. Transfer learning is often useful in such scenarios, resulting in improved performance [3, 4] and faster convergence [5]. Fortunately, there exists some large, publicly available ECG datasets, which enable DNNs to learn important latent features, then transfer the learned knowledge to our main task, typically with much less annotated data. There are two most commonly used transfer learning techniques: head retraining [6, 3] and fine-tuning [7, 8]. Both replace the top classification layer to match the number of target task’s outputs; however, while the former freezes all feature extractor layers and only updates the top layer’s parameters during training on the target dataset, the latter does not have such a constraint and makes all layers trainable. Research suggested that fine-tuning leads to better performance [9, 4], thus it has been accepted as a de facto standard.

Given the effectiveness of fine-tuning, a new problem arises: how do we select the best pre-trained checkpoints among a large candidate pool? A checkpoint is a model pre-trained on a source dataset, with a specific set of hyperparameter settings. It is straightforward to actually do the fine-tuning and then select the top ones; however, this method is obviously expensive and difficult to scale. Transferability estimation [10, 11] aims to address the above bottleneck by developing a metric that indicates how effectively transfer learning can apply to the target task, ideally with minimal interaction with it. Good estimation is likely to facilitate the checkpoint selection process. In the domain of computer vision, several transferability measures were developed. Tran et al. [12] introduced negative conditional entropy between the source and target label sets. Bao et al. [13] proposed a transferability measure called H-score, which was based on solving a Maximal HGR Correlation problem [14, 15, 16]. Nguyen et al. [9] developed LEEP, an efficient estimate with no expensive training on target tasks. However, those measures only apply to multi-class

classification problems, thus cannot be directly applicable to multi-label tasks such as ECG diagnosis, in which a patient may suffer from more than one cardiovascular disease.

Key Contributions:

- We propose MELEP, a transferability measure that can directly apply to multi-label classification problems in automatic ECG interpretation. To the best of our knowledge, we are the first to develop such a measure to estimate the effectiveness of transfer learning in the ECG domain.
- We conducted the first extensive experiment of transfer learning for 12-lead ECG data. We focused on small downstream datasets and covered a wide range of source checkpoints, which were produced from multiple source datasets and representatives of two most popular DNN architectures for time-series analysis: convolutional and recurrent neural networks.

Our article is structured as follows: first, we provide the mathematical foundation behind MELEP and describe the intuition and its properties. Then four 12-lead ECG datasets and two DNN architectures are introduced, which build the backbone of our experiments. We evaluate the ability of MELEP to predict the fine-tuning performance of a convolutional neural network by conducting extensive experiments with multiple checkpoints produced from pretraining the model on different source datasets. To show the versatility of MELEP, we replicate the experiment with a recurrent neural network, affirming that its capability is not tied to a specific model architecture. Next, we demonstrate the effectiveness of MELEP in a real-world scenario, which is selecting the best checkpoints among a group of pre-trained candidates. Finally, we discuss some notable properties, extensions, and applications of MELEP and suggest promising directions for future study.

2. MATERIALS & METHODS

2.1. Multi-Label Expected Log of Empirical Predictions (MELEP)

Consider transfer learning from one multi-label classification task to another.

Let:

- Θ be the pre-trained model on the source task.
- $\mathcal{L}_s = \{0, 1, \dots, \mathcal{Z} - 1\}$ be the source label set of size $|\mathcal{L}_s| = \mathcal{Z}$.
- $\mathcal{L}_t = \{0, 1, \dots, \mathcal{Y} - 1\}$ be the target label set of size $|\mathcal{L}_t| = \mathcal{Y}$.

- $\mathcal{D} = \{(x_1, \mathbf{y}_1), \dots, (x_n, \mathbf{y}_n)\}$ be the target dataset of size n . \mathbf{y}_i is a label vector of size \mathcal{Y} .
- $(y, z) \in \mathcal{L}_t \times \mathcal{L}_s$ be a pair of target-source labels taken from the two sets.
- (t, s) be the values of (y, z) . In the ECG classification context, the label values are binary, so $(t, s) \in \{0, 1\} \times \{0, 1\}$.

then MELEP is computed as follows:

- Step 1: Compute the dummy label distributions of the target data over the source label set, denoted by a vector $\hat{\mathbf{y}}_i = \Theta(x_i)$ of size \mathcal{Z} , by forward passing each data point to the pre-trained model.
- Step 2: Consider each pair of target-source labels (y, z) . Let θ_{iz} denote the value of $\hat{\mathbf{y}}_i$ at the z^{th} column, i.e. the predicted probability that the sample x_i belongs to label z .

1. Compute its 2×2 empirical joint distribution matrix $\hat{\mathbf{P}}_{yz}(t, s)$, with value at row t column s is:

$$\hat{P}_{yz}(t, s) = \frac{1}{n} \sum_{i: y_{iz}=t} (\theta_{iz})_s \tag{1}$$

where $\sum_{i: y_{iz}=t}$ means we select all samples x_i with the z^{th} ground-truth label y_{iz} equal to t . With corresponding values of s , $(\theta_{iz})_1$ and $(\theta_{iz})_0$ are the probabilities that the label z can and cannot be assigned to the sample x_i , respectively.

2. Compute the empirical marginal distribution vector (of size 2) with respect to the source label z :

$$\begin{aligned} \hat{P}_z(s) &= \frac{1}{n} \sum_{i=1}^n (\theta_{iz})_s \\ &= \hat{P}_{yz}(0, s) + \hat{P}_{yz}(1, s) \end{aligned} \tag{2}$$

3. Compute the 2×2 empirical conditional distribution matrix $\hat{\mathbf{P}}_{y|z}(t, s)$ of the target label y given the source label z , with value at row t column s is:

$$\hat{P}_{y|z}(t|s) = \frac{\hat{P}_{yz}(t, s)}{\hat{P}_z(s)} \tag{3}$$

For any input x_i , consider a binary classifier that predicts whether x_i belongs to label y by first randomly drawing \mathcal{Z} dummy labels from $\Theta(x_i)$, then averaging the likelihood of y based on \mathcal{Z} empirical conditional distributions $\hat{\mathbf{P}}_{y|z}$. This process is repeated for all \mathcal{Y} target labels. The set of binary classifiers is called the *Empirical*

Table 1. Statistics of datasets used in this work.

Dataset	Number of records	Number of labels	Sampling rate (Hz)	Duration (sec)
CPSC2018 [17]	6,877	9	500	6-60
PTB-XL [18]	21,837	44	500 & 1000	10
Georgia [19]	10,344	62	500	10
CSN [20, 21]	45,152	94	500	10

Predictor (EP). MELEP is defined as the average negative log-likelihood of the EP across all target labels, as follows:

- Step 3: Compute the Expected Logarithm of Empirical Prediction with respect to the label pair (y, z) :

$$\phi(\Theta, \mathcal{D}, y, z) = -\frac{1}{n} \sum_{i=1}^n \log \left(\sum_{s=0}^1 \hat{P}_{y|z}(y_{iz}|s)(\theta_{iz})_s \right) \quad (4)$$

- Step 4: Compute MELEP by taking the weighted average of $\phi(\theta, \mathcal{D}, y, z)$ over all target-source label pairs:

$$\Phi(\Theta, \mathcal{D}) = \frac{1}{\mathcal{Y}} \sum_y w_y \times \frac{1}{\mathcal{Z}} \sum_z \phi(\Theta, \mathcal{D}, y, z) \quad (5)$$

where w_y are the weights of the target label y in the target dataset, i.e. the ratio of the number of positive samples to the number of negative samples of y . Note that we do not take the source weights into consideration, because in practice, it makes sense to assume that we do not know the source label distribution prior to fine-tuning.

From its definition, MELEP is always positive, and smaller values indicate superior transferability. Intuitively, MELEP can be regarded as a distance metric, indicating how "close" the pre-trained model Θ and the target dataset \mathcal{D} are. The closer the distance, the easier the transfer.

The measure is *generic*, meaning that it can be applied to all types of checkpoints, and works without any prior knowledge of the pre-training process, such as data distribution, hyperparameter settings, optimizer, loss functions, etc. Furthermore, the computation of MELEP is *efficient*, which renders it practically useful. This lightweight property is inherited from the original LEEP [9], with the calculation involving only a single forward pass through the target dataset \mathcal{D} , requiring no training on the downstream task.

2.2. Datasets

We used publicly available 12-lead ECG datasets in this work. The first source was the public training dataset from the China Physiological Signal Challenge 2018 (CPSC2018) [17]. This dataset comprises 6,877 ECG records, each associated with at most nine diagnostic categories: NORM (representing normal ECG patterns), AF (Atrial Fibrillation), I-AVB (First-degree atrioventricular block), LBBB (Left Bundle Branch Block), RBBB (Right Bundle Branch Block), PAC (Premature Atrial Contraction), PVC (Premature ventricular contraction), STD (ST-segment Depression), and STE (ST-segment Elevated).

The second dataset was PTB-XL [18], containing 21,837 records from 18885 patients, and a total of 44 diagnostics statements. The dataset's authors organized these diagnostic labels into a hierarchical structure [22], categorizing the 44 labels into five broader superclasses, namely: NORM (normal ECG), MI (Myocardial Infarction), STTC (ST/T-Changes), HYP (Hypertrophy), and CD (Conduction Disturbance). We followed this structure and focused on these five superclasses when conducting experiments with the PTB-XL dataset.

Our third dataset, known as the Georgia dataset [19], consists of 10,344 ECGs that reflect the demographic characteristics of the Southeastern United States. The data covers a diverse range of 67 unique diagnoses. However, for our research, we focused on a subset of 10 specific labels, which had the most substantial number of samples: NORM, AF, I-AVB, PAC, SB (Sinus Bradycardia), LAD (left axis deviation), STach (Sinus Tachycardia), TAb (T-wave Abnormal), TInv (T-wave Inversion), and LQT (Prolonged QT interval).

The last source was the Chapman University, Shaoxing People's Hospital, and Ningbo First Hospital database [20, 21], which we will refer to as the CSN dataset for brevity. This dataset contains 45,152 12-lead ECG records, each lasting for 10 seconds and sampled at 500 Hz. There are a total of 94 unique labels, among which we focused on 20 labels with more than 1,000 records for our experiments. These 20 labels are SB, NORM, STach, TAb, TInv, AF, STD, LAD, PAC, I-AVB, PVC, AFL (Atrial Flutter), LVH (Left Ventricular Hypertrophy), STC (S-T changes), SA (Sinus Arrhythmia), LQRSV

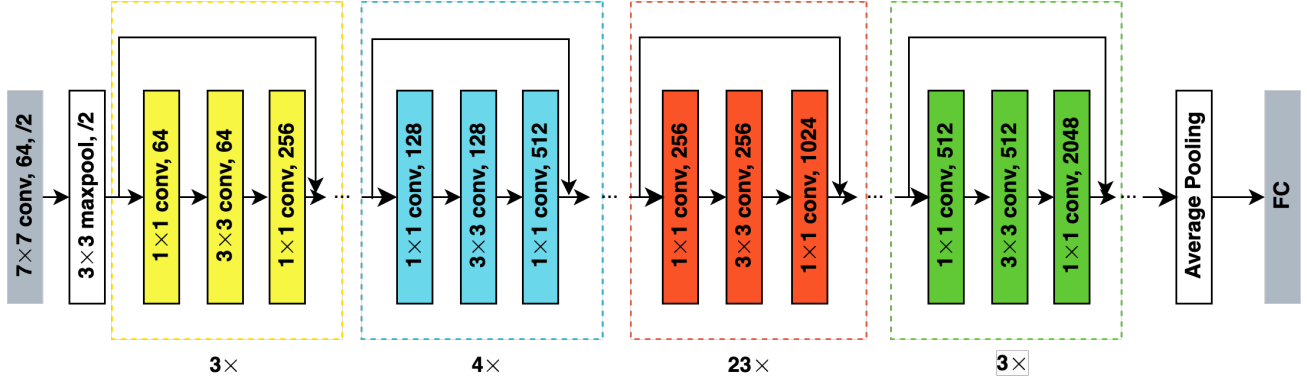


Fig. 1. ResNet1d101 Architecture

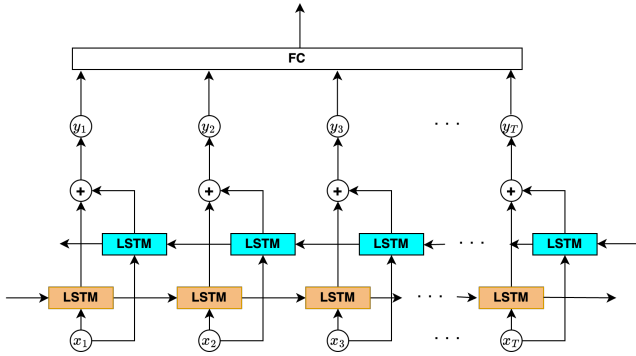


Fig. 2. Bi-LSTM Architecture

(Low QRS Voltages), PR (pacing rhythm), NSTTA (Nonspecific ST-T Abnormality), CRBBB (complete Right Bundle Branch Block), QAb (Q-wave Abnormal).

Table 1 summarizes key statistics of the four data sources. In terms of data preprocessing, we applied the following procedures:

- Downsampling: we reduced the sampling frequency of all ECG records from 500 Hz to 100 Hz. This helps reduce computational load while retaining essential information.
- Cropping: for ECG records longer than the desired duration (ten seconds), we cropped them to meet this target. This step ensures that all records have consistent lengths for training.

It is worth noting that only a tiny fraction of records have durations shorter than ten seconds: six out of 6,877 in the CPSC2018 dataset, 52 out of 10,334 in the Georgia dataset, and none in the PTB-XL and CSN datasets. Therefore, instead of padding these records to meet the desired duration, which could potentially introduce unwanted noise or artifacts into the signals, they were simply omitted from our experiments.

We used the CSN and PTB-XL datasets for fine-tuning due to their relatively large amount of records. When fine-tuning models on the former, we pre-trained our models using three source datasets: CPSC2018, PTB-XL, and Georgia. When fine-tuning on the latter, we only used two source datasets: CPSC2018 and Georgia.

For pretraining, we partitioned each of the source datasets into training and test sets as follows. For PTB-XL, we followed the recommended split in [18], pretraining our models on the first eight folds, and testing on the tenth fold. For the CPSC2018 and Georgia datasets, we kept 33% the amount of data in the test set and allocated the remaining for pretraining.

2.3. Deep Learning Models

We investigated two widely used deep learning architectures for time-series analysis:

- Convolutional Neural Network (CNN): we utilized ResNet1d101, which is a 1D variant of ResNet101 [23]. The architecture of the ResNet1d101 model is illustrated in Figure 1.
- Recurrent Neural Network (RNN): the Bidirectional Long Short Term Memory (Bi-LSTM) architecture [24] was used. The structure of the Bi-LSTM model is visually presented in Figure 2.

Since the source datasets have varying numbers of labels, the last fully-connected layer of the models was adjusted to align with the respective number of outputs. During pretraining, each model was trained on a source training set for 50 epochs, using Adam optimizer [25] with a learning rate of 0.01. At the end of each epoch, we recorded the average F1 score on the test set, which served as an early stopping criterion. We observed that Bi-LSTM experienced overfitting when training beyond the early stopping point, whereas ResNet1d101 mostly

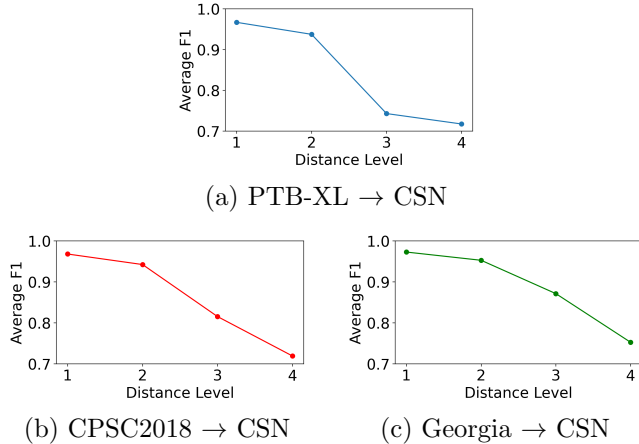


Fig. 3. Relation of MELEP (partitioned as four distance levels) and fine-tuning performance of ResNet1d101 on target tasks sampled from the CSN dataset.

converged.

3. EXPERIMENTS & RESULTS

In this section, we show the potential of MELEP in predicting the performance of fine-tuning a pre-trained model on a target dataset. In practice, transfer learning is often used when dealing with limited human-annotated data. Therefore, we focused on investigating MELEP in the context of small target datasets.

3.1. MELEP vs Average F1 of CNN fine-tuned on CSN

We first experimented with the convolutional model ResNet1d101. This model was pre-trained on three different source datasets: PTB-XL, CPSC2018 and Georgia, as described in Section 2.2, resulting in three respective source checkpoints.

Each source checkpoint was then undergone an experiment with a wide range of target tasks sampled from the CSN dataset. To construct these tasks, we started with the set of 20 labels in the CSN dataset with at least 1000 positive samples, as in Section 2.2. N labels were then randomly sampled without replacement from the set, where N varied from 2 to 10. This step ensured that the target tasks would cover a diverse set of target labels. Records with no positive values for the N selected labels were filtered out to avoid creating a sparse dataset, and to guarantee that every sample left contained at least one positive label. We then randomly select 1000 records among the remaining to form a data fold. The process was repeated 100 times to generate a total of 100 data folds for our experiment.

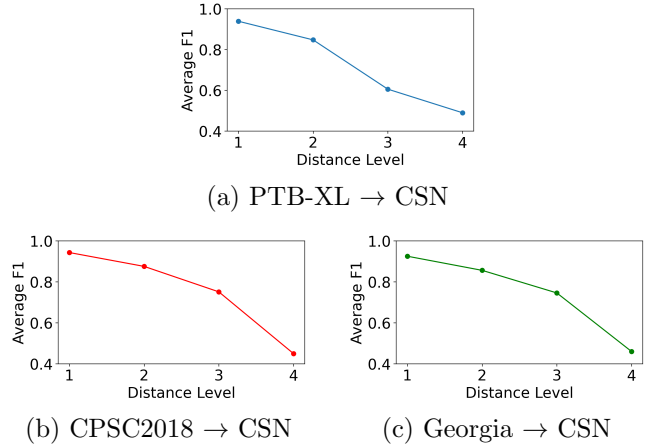


Fig. 4. Relation of MELEP (partitioned as four distance levels) and fine-tuning performance of Bi-LSTM on target tasks sampled from the CSN dataset.

For each fold, we further split it into training and test subsets with a 7:3 ratio, i.e. 700 training records and 300 test records. Subsequently, we compute MELEP using the pre-trained checkpoint and the training subset only, following the algorithm described in Section 2.1. Prior to fine-tuning the model, we replaced the top fully connected layer of the checkpoint, adjusting the number of output neurons to match the target number of labels N . The entire modified model was then fine-tuned on the training subset for 50 epochs with early stopping, using Adam optimizer [25]. To evaluate the fine-tuning performance, we recorded the weighted average F1-score across the N labels of the given fold. F1-score was chosen as the evaluation metric due to its robustness in handling class imbalances [26], a common feature of ECG data, compared to accuracy. Ultimately, we gathered 100 points of (MELEP, average F1) representing the correlation between MELEP and the fine-tuning performance of the source checkpoint across a wide range of target tasks.

We performed a correlation analysis between MELEP and target performance, following a similar approach used in assessing transferability on multi-class computer vision tasks [27, 9]. The first three rows in Table 2 show the results of the three ResNet1d101 checkpoints in this experiment, revealing strong negative correlations between MELEP and average F1 scores, all of which are below -0.6 . To visualize this relationship, Figure 3 classifies the MELEP values into four distinct distance levels. Within each level, we calculated the mean of average F1 scores from all the folds with MELEP falling into that level. The lower the MELEP, the closer the distance, implying easier transferability.

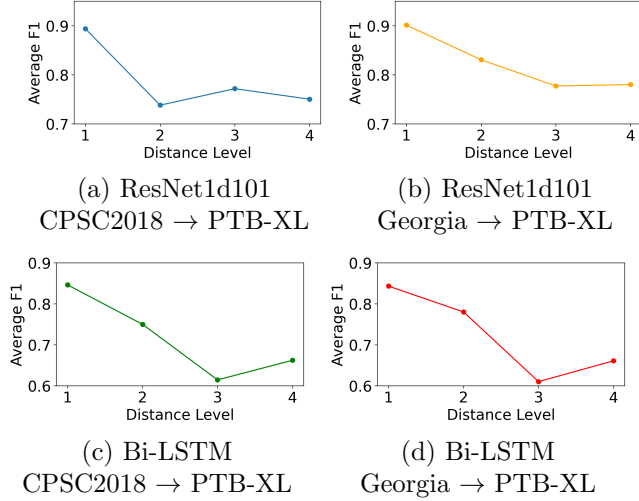


Fig. 5. Relation of MELEP (partitioned as four distance levels) and fine-tuning performance of ResNet1d101 and Bi-LSTM on target tasks sampled from the PTB-XL dataset.

3.2. MELEP vs Average F1 of RNN fine-tuned on CSN

To illustrate the applicability of MELEP to RNN, we repeated the experiment in Section 3.1 with Bi-LSTM as the source model. Similar to ResNet1d101, the Bi-LSTM model was pre-trained on three source datasets: PTB-XL, CPSC2018, and Georgia. We leveraged the same set of 100 CSN data folds which were previously constructed for the CNN experiment, and applied the identical fine-tuning procedure.

In Table 2 (specifically, the first three rows of the Bi-LSTM section), we observe a robust correlation, even stronger than that observed with ResNet1d101, between MELEP and average F1 scores. This correlation is visually depicted in Figure 4, where MELEP is categorized into the same distance levels as described in Section 3.1. The trend remains consistent: the closer the distance, the better the transfer.

3.3. MELEP vs Average F1 of Models fine-tuned on PTB-XL

In this experiment, we explored the use of MELEP on a different target dataset, specifically PTB-XL, chosen for its relatively large amount of records. We followed the same procedure outlined in Section 3.1 to construct 100 target data folds, with the only difference being the number of labels N . These label sets ranged from two to five and were derived from the five superclasses covering the whole PTB-XL dataset, as described in Section 2.2.

We considered four different checkpoints: ResNet1d101

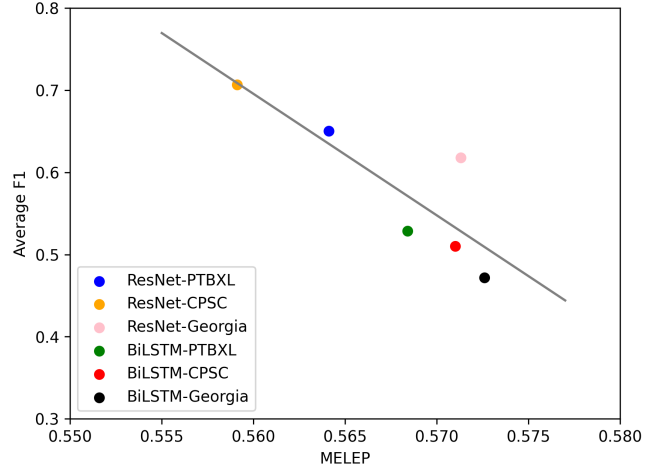


Fig. 6. MELEP for checkpoint selection problem.

and Bi-LSTM models pre-trained on the CPSC2018 and Georgia datasets. The results in Table 2 indicate a moderate correlation between MELEP and transfer performance, with most correlation coefficients below -0.5 . These correlations, while still significant, are slightly weaker than what was observed in the experiment with the CSN dataset (Section 3.1 and 3.2), as shown in Figure 5, where the predictive trend of MELEP is disrupted, with an increase instead of a decrease at one distance level (the 2nd level for ResNet1d101 pre-trained on CPSC2018 and the 3rd level for other checkpoints).

3.4. MELEP for Checkpoint Selection

This experiment demonstrates the use of MELEP in practice to effectively estimate fine-tuning performance in a multi-label classification task, before the actual fine-tuning process takes place. Consider a checkpoint selection problem, where the goal is to choose the best candidate from a set of given source checkpoints for a target task.

In this scenario, we had six candidate checkpoints: ResNet1d101-PTBXL, ResNet1d101-CPSC, ResNet1d101-Georgia, BiLSTM-PTBXL, BiLSTM-CPSC, BiLSTM-Georgia. To simulate the context of fine-tuning of a small target dataset, the target task was generated following the random process outlined in Section 3.1, with the target fold being 1000 records sampled from the CSN dataset, belonging to 8 labels: PAC, PVC, TAB, PR, TInv, IAVB, AFL and CRBBB. Subsequently, we divided this fold into training and test subsets with a 7:3 ratio. The training subset was used for computing MELEP and fine-tuning, while the test set was reserved for performance evaluation.

In Figure 6, MELEP values and their correspond-

Table 2. Pearson correlation coefficients between MELEP and average of F1-scores in the experiments described in Section 3.1, 3.2 and 3.3. Strong negative correlations were observed for most cases, indicating MELEP’s potential to predict fine-tuning performance with only a single forward pass required.

Model	Source Data	Target Data	Details in	Correlation Coefficient
ResNet1d101	PTB-XL	CSN	Sec. 3.1	-0.639
	CPSC2018	CSN	Sec. 3.1	-0.631
	Georgia	CSN	Sec. 3.1	-0.608
	CPSC2018	PTB-XL	Sec. 3.3	-0.476
	Georgia	PTB-XL	Sec. 3.3	-0.500
Bi-LSTM	PTB-XL	CSN	Sec. 3.2	-0.691
	CPSC2018	CSN	Sec. 3.2	-0.670
	Georgia	CSN	Sec. 3.2	-0.665
	CPSC2018	PTB-XL	Sec. 3.3	-0.551
	Georgia	PTB-XL	Sec. 3.3	-0.517

ing average F1 scores for all six source checkpoints are displayed, along with the reference best-fit line. The graph clearly illustrates the effectiveness of MELEP in predicting the performance of the given checkpoints on the target task. Notably, the checkpoint with the lowest MELEP, ResNet1d101 pre-trained on the CPSC2018 dataset, achieved the highest average F1 score. The pattern remains consistent for most checkpoints, with the only outlier of ResNet1d101-Georgia, which had higher MELEP but performed better than two of the Bi-LSTM checkpoints.

4. DISCUSSIONS & CONCLUSION

We introduced MELEP, a novel transferability measure that is directly applicable to multi-label ECG diagnosis. The measure is built upon the foundation of LEEP [9], adapting from single-label multi-class problems in computer vision to multi-label binary-class ones in the ECG domain. We conducted extensive experiments to empirically illustrate the effectiveness of MELEP in predicting the performance of transfer learning in various ECG classification tasks. In this section, we discuss some notable properties, extensions, and applications of MELEP alongside promising directions for future study.

Source model dependence: MELEP computation is based on a source checkpoint, which is a source model pre-trained on a source task. Additionally, MELEP *indirectly* considers the input features when computing the dummy label distributions. Consequently, the score is inherently influenced by the architectural choice, set of hyperparameters, training configurations (such as learning rate, optimizer, dropout rate, etc.), and the performance of the source model.

Source data dependence: in addition, MELEP is also dependent on the source dataset. Equations 4 and

5 show that the cardinality of the source label set contributes to MELEP score. Although MELEP calculation does not require specific label values, it is reasonable to assume that if there is a significant overlap between the source and target label sets, the checkpoint pre-trained on the source task is likely to perform well on the target task.

Considerable extensions: as mentioned in Section 2.1, Equation 5, we do not consider source label weights in the MELEP formula. This exclusion is based on the assumption that we lack prior knowledge of the source label distribution used in pretraining. However, in situations where this information is known, it is more sensible to take the source weights into account. Additionally, there is another variant that deserves consideration for its practical versatility. Instead of aggregating the weighted average of $\phi(\theta, \mathcal{D}, y, z)$ into a single value as in Equation 5, we can output a vector of size \mathcal{Y} , indicating the transferability measures for each target label. Such an approach is well-suited in scenarios where the performances on certain labels hold more significance than others.

Potential applications: apart from the source checkpoint selection use case demonstrated in Section 3.4, MELEP can be useful for continual learning algorithms that based on neural architectures changes or selection of data points in replay buffers [28, 29], facilitating the decision-making process. Furthermore, multi-task learning [30, 31], which often depends on the selection of deep parameter-sharing networks and a combination of task labels, can also benefit from MELEP. Finally, MELEP holds the potential to assist in the selection of hyperparameters for Bayesian optimization [32]. We leave these directions for future work.

5. REFERENCES

- [1] Awni Y Hannun, Pranav Rajpurkar, Mousumeh Haghpanahi, Geoffrey H Tison, Codie Bourn, Mintu P Turakhia, and Andrew Y Ng, “Cardiologist-level arrhythmia detection and classification in ambulatory electrocardiograms using a deep neural network,” *Nature medicine*, vol. 25, no. 1, pp. 65–69, 2019.
- [2] Antônio H Ribeiro, Manoel Horta Ribeiro, Gabriela MM Paixão, Derick M Oliveira, Paulo R Gomes, Jéssica A Canazart, Milton PS Ferreira, Carl R Andersson, Peter W Macfarlane, Wagner Meira Jr, et al., “Automatic diagnosis of the 12-lead ecg using a deep neural network,” *Nature communications*, vol. 11, no. 1, pp. 1760, 2020.
- [3] Ali Sharif Razavian, Hossein Azizpour, Josephine Sullivan, and Stefan Carlsson, “Cnn features off-the-shelf: an astounding baseline for recognition,” in *Proceedings of the IEEE conference on computer vision and pattern recognition workshops*, 2014, pp. 806–813.
- [4] Simon Kornblith, Jonathon Shlens, and Quoc V Le, “Do better imagenet models transfer better?,” in *Proceedings of the IEEE/CVF conference on computer vision and pattern recognition*, 2019, pp. 2661–2671.
- [5] Kaiming He, Ross Girshick, and Piotr Dollár, “Rethinking imagenet pre-training,” in *Proceedings of the IEEE/CVF International Conference on Computer Vision*, 2019, pp. 4918–4927.
- [6] Jeff Donahue, Yangqing Jia, Oriol Vinyals, Judy Hoffman, Ning Zhang, Eric Tzeng, and Trevor Darrell, “Decaf: A deep convolutional activation feature for generic visual recognition,” in *International conference on machine learning*. PMLR, 2014, pp. 647–655.
- [7] Jason Yosinski, Jeff Clune, Yoshua Bengio, and Hod Lipson, “How transferable are features in deep neural networks?,” *Advances in neural information processing systems*, vol. 27, 2014.
- [8] Sinno Jialin Pan and Qiang Yang, “A survey on transfer learning,” *IEEE Transactions on knowledge and data engineering*, vol. 22, no. 10, pp. 1345–1359, 2009.
- [9] Cuong Nguyen, Tal Hassner, Matthias Seeger, and Cedric Archambeau, “Leap: A new measure to evaluate transferability of learned representations,” in *International Conference on Machine Learning*. PMLR, 2020, pp. 7294–7305.
- [10] Haitham Bou Ammar, Eric Eaton, Matthew E Taylor, Decebal Constantin Mocanu, Kurt Driessens, Gerhard Weiss, and Karl Tuyls, “An automated measure of mdp similarity for transfer in reinforcement learning,” in *Workshops at the twenty-eighth AAAI conference on artificial intelligence*, 2014, vol. 1.
- [11] Jivko Sinapov, Sanmit Narvekar, Matteo Leonetti, and Peter Stone, “Learning inter-task transferability in the absence of target task samples,” in *Proceedings of the 2015 International Conference on Autonomous Agents and Multiagent Systems*, 2015, pp. 725–733.
- [12] Anh T Tran, Cuong V Nguyen, and Tal Hassner, “Transferability and hardness of supervised classification tasks,” in *Proceedings of the IEEE/CVF International Conference on Computer Vision*, 2019, pp. 1395–1405.
- [13] Yajie Bao, Yang Li, Shao-Lun Huang, Lin Zhang, Lizhong Zheng, Amir Zamir, and Leonidas Guibas, “An information-theoretic approach to transferability in task transfer learning,” in *2019 IEEE international conference on image processing (ICIP)*. IEEE, 2019, pp. 2309–2313.
- [14] Hermann O Hirschfeld, “A connection between correlation and contingency,” in *Mathematical Proceedings of the Cambridge Philosophical Society*. Cambridge University Press, 1935, vol. 31, pp. 520–524.
- [15] Hans Gebelein, “Das statistische problem der korrelation als variations-und eigenwertproblem und sein zusammenhang mit der ausgleichsrechnung,” *ZAMM-Journal of Applied Mathematics and Mechanics/Zeitschrift für Angewandte Mathematik und Mechanik*, vol. 21, no. 6, pp. 364–379, 1941.
- [16] Alfréd Rényi, “On measures of dependence,” *Acta mathematica hungarica*, vol. 10, no. 3-4, pp. 441–451, 1959.
- [17] Feifei Liu, Chengyu Liu, Lina Zhao, Xiangyu Zhang, Xiaoling Wu, Xiaoyan Xu, Yulin Liu, Caiyun Ma, Shoushui Wei, Zhiqiang He, et al., “An open access database for evaluating the algorithms of electrocardiogram rhythm and morphology abnormality detection,” *Journal of Medical Imaging and Health Informatics*, vol. 8, no. 7, pp. 1368–1373, 2018.
- [18] Patrick Wagner, Nils Strodthoff, Ralf-Dieter Bouseljelot, Dieter Kreiseler, Fatima I Lunze, Wojciech Samek, and Tobias Schaeffter, “Ptb-xl, a large publicly available electrocardiography dataset,” *Scientific data*, vol. 7, no. 1, pp. 154, 2020.

- [19] Erick A Perez Alday, Annie Gu, Amit J Shah, Chad Robichaux, An-Kwok Ian Wong, Chengyu Liu, Feifei Liu, Ali Bahrami Rad, Andoni Elola, Salman Seyedi, et al., “Classification of 12-lead eegs: the physionet/computing in cardiology challenge 2020,” *Physiological measurement*, vol. 41, no. 12, pp. 124003, 2020.
- [20] Jianwei Zheng, Jianming Zhang, Sidy Danioko, Hai Yao, Hangyuan Guo, and Cyril Rakovski, “A 12-lead electrocardiogram database for arrhythmia research covering more than 10,000 patients,” *Scientific data*, vol. 7, no. 1, pp. 48, 2020.
- [21] Jianwei Zheng, Huimin Chu, Daniele Struppa, Jianming Zhang, Sir Magdi Yacoub, Hesham El-Askary, Anthony Chang, Louis Ehwerhemuepha, Islam Abudayyeh, Alexander Barrett, et al., “Optimal multi-stage arrhythmia classification approach,” *Scientific reports*, vol. 10, no. 1, pp. 2898, 2020.
- [22] Nils Strodthoff, Patrick Wagner, Tobias Schaeffter, and Wojciech Samek, “Deep learning for ecg analysis: Benchmarks and insights from ptb-xl,” *IEEE Journal of Biomedical and Health Informatics*, vol. 25, no. 5, pp. 1519–1528, 2020.
- [23] Kaiming He, Xiangyu Zhang, Shaoqing Ren, and Jian Sun, “Deep residual learning for image recognition,” in *Proceedings of the IEEE conference on computer vision and pattern recognition*, 2016, pp. 770–778.
- [24] Sepp Hochreiter and Jürgen Schmidhuber, “Long short-term memory,” *Neural computation*, vol. 9, no. 8, pp. 1735–1780, 1997.
- [25] Diederik P Kingma and Jimmy Ba, “Adam: A method for stochastic optimization,” *arXiv preprint arXiv:1412.6980*, 2014.
- [26] László A Jeni, Jeffrey F Cohn, and Fernando De La Torre, “Facing imbalanced data—recommendations for the use of performance metrics,” in *2013 Humaine association conference on affective computing and intelligent interaction*. IEEE, 2013, pp. 245–251.
- [27] Anh T Tran, Cuong V Nguyen, and Tal Hassner, “Transferability and hardness of supervised classification tasks,” in *Proceedings of the IEEE/CVF International Conference on Computer Vision*, 2019, pp. 1395–1405.
- [28] German I Parisi, Ronald Kemker, Jose L Part, Christopher Kanan, and Stefan Wermter, “Continual lifelong learning with neural networks: A review,” *Neural networks*, vol. 113, pp. 54–71, 2019.
- [29] Dani Kiyasseh, Tingting Zhu, and David Clifton, “A clinical deep learning framework for continually learning from cardiac signals across diseases, time, modalities, and institutions,” *Nature Communications*, vol. 12, no. 1, pp. 4221, 2021.
- [30] Jinlong Ji, Xuhui Chen, Changqing Luo, and Pan Li, “A deep multi-task learning approach for ecg data analysis,” in *2018 IEEE EMBS International Conference on Biomedical & Health Informatics (BHI)*. IEEE, 2018, pp. 124–127.
- [31] Ming-En Hsieh and Vincent Tseng, “Boosting multi-task learning through combination of task labels-with applications in ecg phenotyping,” in *Proceedings of the AAAI Conference on Artificial Intelligence*, 2021, vol. 35, pp. 7771–7779.
- [32] Hongqiang Li, Zifeng Lin, Zhixuan An, Shasha Zuo, Wei Zhu, Zhen Zhang, Yuxin Mu, Lu Cao, and Juan Daniel Prades Garcia, “Automatic electrocardiogram detection and classification using bidirectional long short-term memory network improved by bayesian optimization,” *Biomedical Signal Processing and Control*, vol. 73, pp. 103424, 2022.